RESEARCH ARTICLE

JOR *Spine* OPEN ACCESS

Percutaneous lumbar annular puncture: A rat model to study intervertebral disc degeneration and pain-related behavior

Richard A. Wawrose[1] | Brandon K. Couch[1] | Malcom Dombrowski[1] |
Stephen R. Chen[1] | Anthony Oyekan[1] | Qing Dong[1] | Dong Wang[1] |
Chaoming Zhou[1] | Joseph Chen[1] | Karthik Modali[1] | Marit Johnson[1] |
Zachary Sedor-Schiffhauer[1] | T. Kevin Hitchens[2] | Tao Jin[2] | Kevin M. Bell[1] |
Joon Y. Lee[1] | Gwendolyn A. Sowa[1,3] | Nam V. Vo[1]

[1]Ferguson Laboratory for Orthopaedic and Spine Research, Department of Orthopaedic Surgery, University of Pittsburgh, Pittsburgh, Pennsylvania, USA

[2]Animal Imaging Center, University of Pittsburgh, Pittsburgh, Pennsylvania, USA

[3]Department of Physical Medicine and Rehabilitation, University of Pittsburgh, Pittsburgh, Pennsylvania, USA

Correspondence
Nam V. Vo, Ferguson Laboratory for Orthopaedic and Spine Research, Department of Orthopaedic Surgery, University of Pittsburgh, 200 Lothrop Street, E1644 Biomedical Science Tower, Pittsburgh, PA 15261, USA.
Email: nvv1@pitt.edu

Funding information
National Institutes of Health, Grant/Award Number: R01 AG044376-01; Pittsburgh Foundation

Abstract

Background: Previous animal models of intervertebral disc degeneration (IDD) rely on open surgical approaches, which confound the degenerative response and pain behaviors due to injury to surrounding tissues during the surgical approach. To overcome these challenges, we developed a minimally invasive percutaneous puncture procedure to induce IDD in a rat model.

Methods: Ten Fischer 344 male rats underwent percutaneous annular puncture of lumbar intervertebral discs (IVDs) at L2-3, L3-4, and L4-5. Ten unpunctured rats were used as controls. Magnetic resonance imagings (MRIs), serum biomarkers, and behavioral tests were performed at baseline and 6, 12, and 18 weeks post puncture. Rats were sacrificed at 18 weeks and disc histology, immunohistochemistry, and glycosaminoglycan (GAG) assays were performed.

Results: Punctured IVDs exhibited significant reductions in MRI signal intensity and disc volume. Disc histology, immunohistochemistry, and GAG assay results were consistent with features of IDD. IVD-punctured rats demonstrated significant changes in pain-related behaviors, including total distance moved, twitching frequency, and rearing duration.

Conclusions: This is the first reported study of the successful establishment of a reproducible rodent model of a percutaneous lumbar annular puncture resulting in discogenic pain. This model will be useful to test therapeutics and elucidate the basic mechanisms of IDD and discogenic pain.

KEYWORDS
intervertebral disc degeneration, low back pain, percutaneous annular puncture, rat model

---

Richard A. Wawrose and Brandon K. Couch contributed equally to this manuscript.

(A)

(B)

1 | INTRODUCTION

Low back pain (LBP) is a leading cause of disability worldwide with 80% of adults in the United States experiencing at least one episode within their lifetime.[1,2] Low back pain is a heavy burden on global society, with annual health-care costs exceeding 100 billion dollars in the United States alone.[3–7] Discogenic back pain has been identified as the primary source of pain in approximately 40% of LBP patients.[8,9] Consequently, substantial research has centered on characterizing the pathologic processes contributing to intervertebral disc degeneration (IDD).[10,11]

Various animal models of IDD have been described, with rodent models commonly employed due to low cost, ease of genetic manipulation, and abundant biological research resources.[12–14] In rats, both lumbar and caudal (tail) intervertebral discs (IVDs) have been used to model IDD.[15–21] While caudal discs are accessible without significant surgical exposure, it is unclear whether they can reliably model the biologic environment of the lumbar spine.[12,15–18] Current rat models of the lumbar spine rely on open surgical approaches to expose the vertebral column.[19–26] Although these techniques allow for direct visualization of the IVD, they require large incisions and extensive dissections through the abdominal cavity or paraspinal musculature. These procedures can also result in pain and inflammation of non-disc tissues at the surgical site, which can confound IDD progression. It also makes it difficult to correlate IDD with postoperative pain-related behaviors, which is necessary to evaluate the effect of treatment and therapeutics.

The purpose of this study was to develop a minimally invasive needle puncture procedure to induce lumbar IDD in rats and to determine measurable, pain-associated behavioral changes that will provide utility in the assessment of the efficacy of future therapeutics in treating discogenic LBP. We hypothesized that this percutaneous procedure would result in quantifiable lumbar IDD with pain-associated behavioral changes while minimizing non-disc morbidity associated with open approaches.

2 | METHODS

All procedures were approved by the Institutional Animal Care and Use Committee of the University of Pittsburgh.

2.1 | Experimental animals

Twenty male Fischer 344 rats were housed, two rats per cage with control and experimental rats housed in separate cages. Ten experimental rats underwent a percutaneous puncture procedure of the L2/L3, L3/L4, and L4/L5 IVDs. L1/L2, L5/L6, and L6/S1 IVDs remained unpunctured as internal controls within the experimental group. Ten rats remained unpunctured as a control group, with no discs in these animals undergoing annular puncture (Figure 1). Seven rats were included as sham surgery controls with the skin and soft-tissue puncture with the needle abutting the vertebral body and then withdrawing without puncturing any discs. The average age of the experimental animals at the time of the procedure was
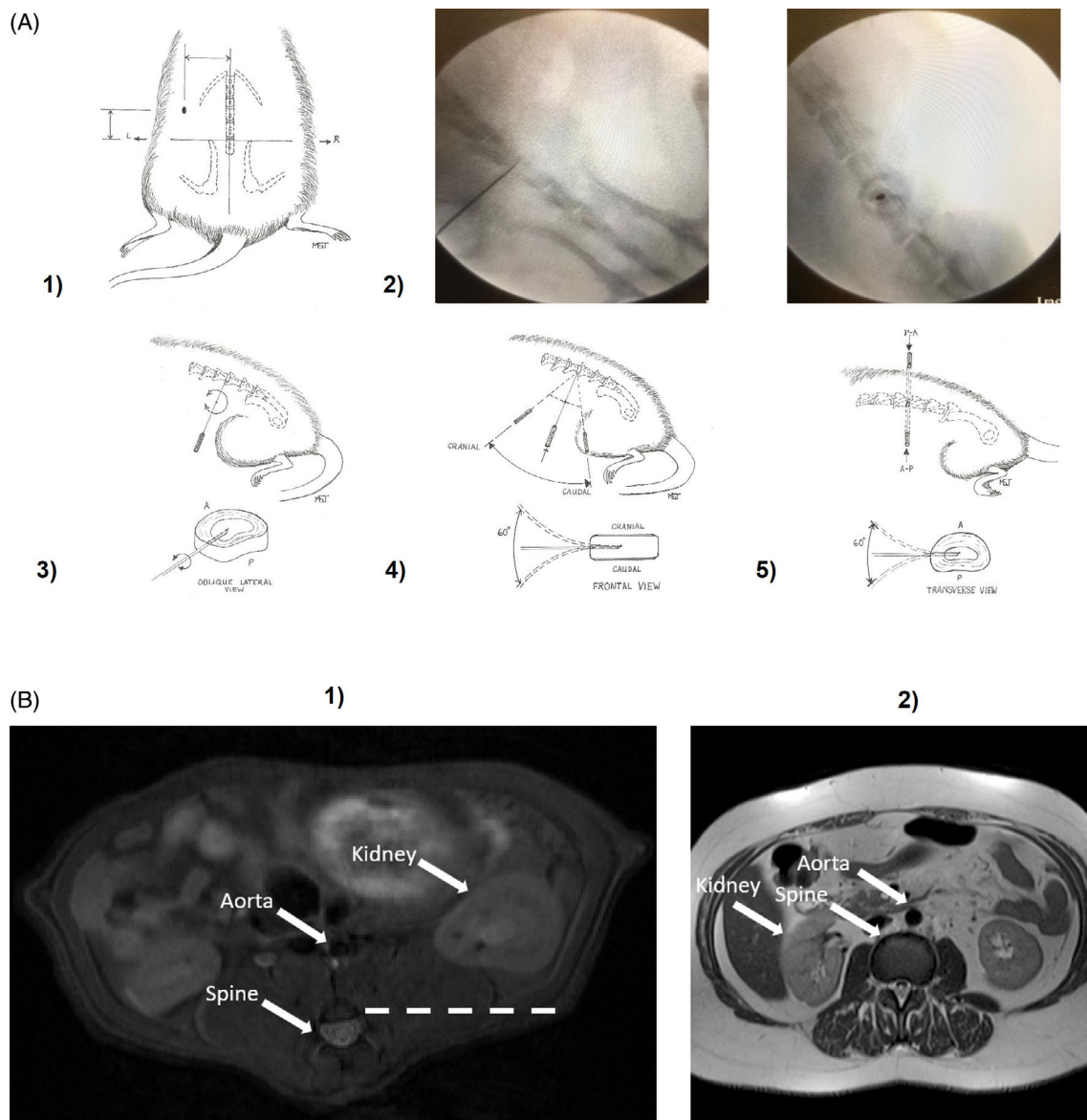
FIGURE 2 Percutaneous lumbar annular puncture procedure (A) and comparison of MRI imaging of rat and human anatomy at the lumbar region (B). (A.1) Starting point identified 3 cm left of the midline and 1.5 cm rostral to a line connecting the iliac crests. (A.2) AP (left) and lateral (right) fluoroscopic images confirming needle puncture into intervertebral disc space. Following fluoroscopic confirmation of proper needle placement, the needle tip is (A.3) rotated 360° around its longitudinal access, then swung 60 degrees in a (A.4) cranial-caudal and (A.5) anterior–posterior direction. (B) Axial T2 MRI imaging of a rat at the level of the L3 vertebra (B.1) and a human at the level of the L2 vertebra (B.2) demonstrating the location of the kidneys and aorta in relationship to the spine. The described path of the needle puncture is indicated by the dotted line. AP, anteroposterior; MRI, magnetic resonance imaging

7.5 ± 0.2 months. Male rats were chosen due to less behavioral variability in response to stressors when compared to female counterparts.[27] Animals were sacrificed 19–24 weeks post puncture, and their entire spines were immediately dissected and flash frozen in liquid nitrogen for storage at −80°C for later analyses (Figure 1).

2.2 | Percutaneous lumbar annular puncture

General anesthesia was induced by inhaled isoflurane, followed by an intraperitoneal injection of 0.1 ml/100 g ketamine HCl (100 mg/ml

Ketamine HCl; Henry Schein Animal Health). Following anesthesia, rats were positioned prone and the hair over the dorsal aspect of the lumbar spine and flanks was shaved. Using a marking pen, a line was drawn connecting the iliac crests, indicating the approximate level of the L5/L6 disc space. A second line was drawn along the midline, connecting the spinous processes. The starting point was marked 1.5 cm rostral to the line connecting the iliac crests and 3 cm lateral to the midline (Figure 2A.1). Punctures were made from the animals' left side to avoid injury to the liver. Chloraprep (BD) was used to sterilize the surgical site.

A sterile 23-gauge needle was inserted through the marked starting point and advanced toward the L4/L5 disc space until
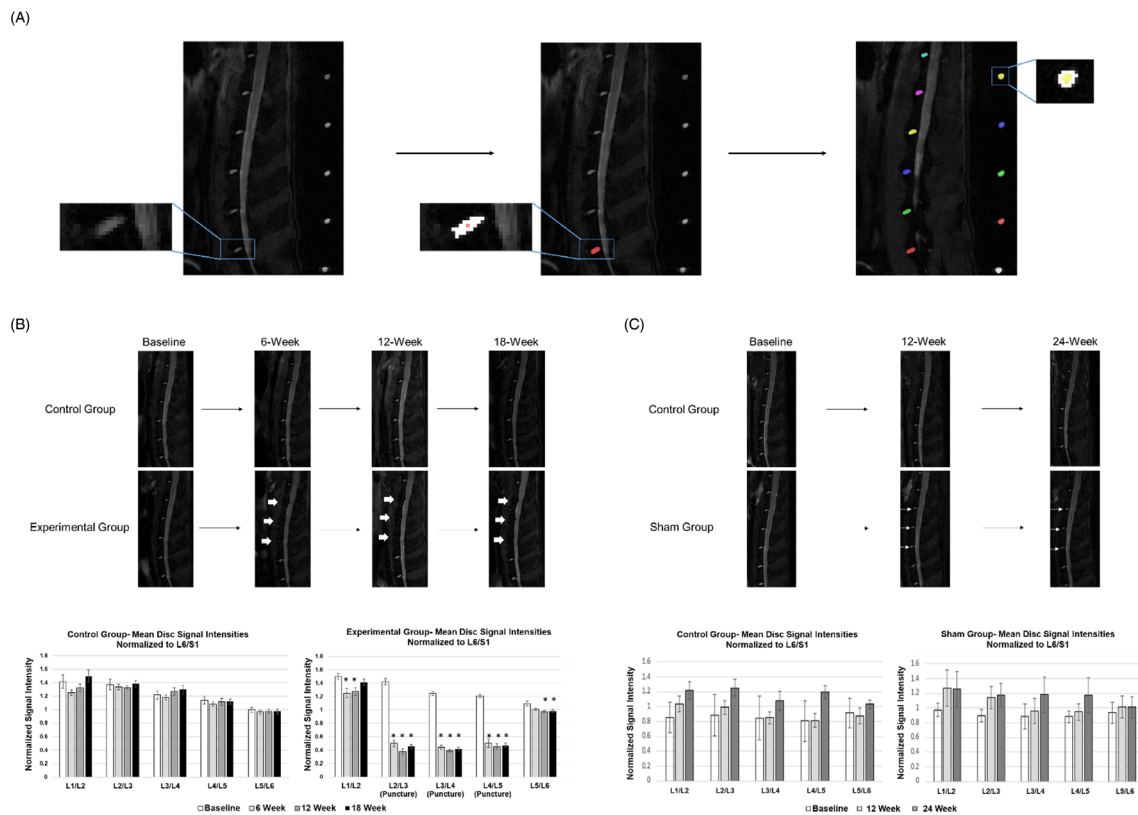
FIGURE 3   T2 MRI of rat spines. (A) The process used for quantifying disc signal intensity. Individual pixels of each NP were highlighted (middle), and signal intensity was quantified using DSI Studio software. This process was repeated for each "phantom" marker isointense to water (right), and average disc intensity values were standardized to the nearest average phantom intensity in order to account for spatial intensity variability based on the location of the disc in relation to the MRI coil. (B) Representative mid-sagittal T2 MRI images from a control and experimental animal at baseline and 6, 12, and 18 weeks post puncture. A decrease in disc signal intensity in the punctured discs (arrows) is noted. Mean disc signal intensities after normalization to mean L6/S1 value are shown in the control and experimental groups at each timepoint. Asterisks represent a significant difference ($p < 0.05$) in mean intensity at indicated timepoint when compared to baseline for a given disc. There were no significant differences between groups at any timepoint in the unpunctured discs (L1/L2 and L5/L6), or baseline in the punctured discs (L2/L3, L3/L4, and L4/L5). There was a significant difference between groups at all postoperative timepoints in the punctured discs ($p < 0.001$). Error bars represent one standard error. (C) Sham control rats exhibited no MRI evidence of IDD. Representative mid-sagittal T2 MRI images from a control and sham surgical animal at baseline, 12, and 24 weeks post surgery. L2–L3, L3–L4, and L4–L5 discs corresponding to the levels of punctured discs in experimental rats are noted (arrows). Graphs represent the mean disc signal intensities after normalization to the mean L6/S1 value in the control and experimental groups at each timepoint. There were no significant differences between groups at any timepoint in the lumbar discs of control and sham rats. Error bars represent one standard error. IDD, intervertebral disc degeneration; MRI, magnetic resonance imaging; NP, nucleus pulposus

increased resistance was encountered. At this point, an anteroposterior (AP) fluoroscopic image was obtained using the Fluoroscan Premier Mini C-arm imaging system (Hologic) to confirm that the needle abutted the vertebral column at the L4/L5 disc space. Guided by fluoroscopy, the needle was then advanced through the annulus fibrosus (AF) into the nucleus pulposus (NP) until the needle tip abutted the contralateral side of the AF. AP fluoroscopic images were obtained to confirm that the needle tip abutted the contralateral AF, and lateral fluoroscopic images were obtained to confirm that the needle did not lie anterior or posterior to the L4/L5 disc space (Figure 2A.2). The needle was rotated 360° five times (Figure 2A.3). Without redirecting the needle, the distal tip was swung 60° five times in a cranial-caudal direction (Figure 2A.4) and 60° five times in an anteroposterior direction (Figure 2A.5) to induce disc injury. The needle was then removed from

the animal. The above procedure was repeated for the L3/L4 and L2/L3 IVDs with each subsequent starting point approximately 1 cm cranial to the previous starting point. Following the procedure, rats were monitored for recovery from anesthesia. Rats were monitored daily for postoperative complications. Sham surgery was also performed in which the needle was inserted into the rat in the same manner as described above until it abutted the vertebral body at the L4/L5 disc space, then the needle was withdrawn from the animal.

The lateral starting point avoids injury to major structures. Unlike in humans, where paraspinal musculature is predominantly posterior to the spine, the paraspinal musculature of rats circumferentially surrounds the spine (Figure 2B). As a result, the intraperitoneal structures and the kidneys are more anterior in rats than in humans and do not obstruct access to the discs laterally. Furthermore, in humans, the aorta

lies directly anterior to the vertebra, while in rats, the aorta is separated from the vertebra by the anterior aspect of the paraspinal muscles.

2.3 | Magnetic resonance imaging

In vivo magnetic resonance imaging (MRI) was performed at preoperative baseline as well as 6, 12, 18, and 24 weeks postoperatively. Rats were anesthetized with 2% isoflurane in a mixture of 30% O_2 and 70% medical air and then positioned supine on an animal bed with a custom Acrylonitrile Butadiene Styrene 3D-printed spine holder. The holder anatomically cradled the spine in a linear orientation, with water-filled polyethylene tubing PE160 (Becton Dickinson), at 1-cm increments under the spine as an MRI reference. Anesthesia was maintained by 1.5% isoflurane via a nose cone. Respiration and temperature were monitored continuously, and the temperature was maintained by a warm animal heating system (SA Instruments). Magnetic resonance imaging was performed on a 9.4 T/30-cm AVIII HD spectrometer (Bruker Biospin) equipped with a 12-cm high-performance gradient set and using an 86-mm quadrature RF transmit volume coil and ParaVision 6.0.1. Following pilot scans, T2-weighted images were acquired using a RARE (Rapid Acquisition with Relaxation Enhancement) sequence in the sagittal plane bisecting the spine, with the following parameters: repetition time (TR)/echo time (TE) = 4000/40 ms, field of view (FOV) = 51.2 × 51.2 mm, acquisition matrix = 256 × 256, five slices with a slice thickness of 0.8 mm, eight averages, and a RARE factor = 8.[28] DSI Studio (http://dsi-studio.labsolver.org) was used to quantify voxel signal intensities (Figure 3A). Regions of interest were manually drawn encompassing each disc to determine the mean disc signal intensity. Disc intensity

values were normalized to the nearest reference water phantom to account for any potential spatial intensity variability based on the location of the disc in relation to the MRI coil. Normalized L1/L2, L2/L3, L3/L4, L4L/5, and L5/L6 values were then indexed to the L6/S1 disc value in the same scan and reported as a mean ± standard error. The average intensity measures for each disc at each timepoint were compared to baseline values to evaluate for disc degeneration. These values were also compared between groups at each timepoint (i.e. puncture L2/L3 to control L2/L3 at 6 weeks).

2.4 | Behavioral assessments

Testing to assess pain-related behaviors was performed prior to annular puncture and at 1, 6, 12, and 18 weeks post puncture. All tests were performed in a black 60 × 60 cm open-field enclosure. Prior to the behavioral test at each timepoint, animals were placed individually in the open-field enclosure for 10 min per day for five consecutive days to acclimate to the testing environment. For the behavioral test, animals were placed individually in the open-field enclosure for a period of 10 min. A camera positioned 6 feet above the enclosure continuously recorded animal movement from a bird's-eye view, consistent with previous literature.[29] Overhead lighting was consistent between trials. All trials were conducted during the late morning hours of the last day of the week at each timepoint. Investigators stood outside of the testing room to minimize external disturbances. Ethovision XT Automated Behavior Recognition software (Noldus Information Technology) tracked and analyzed 23 parameters of animal motion.[30-32] A principal component analysis was used to identify distinct domains of related parameters with

TABLE 1 Behavioral parameters grouped based on the principal component analysis

	Domain 1	Domain 2	Domain 3	Domain 4	Domain 5	Domain 6
Parameter included in regression	Total distance moved	Supported rearing duration	Unsupported rearing duration	Twitching frequency	Grooming duration	Grooming frequency
Associated parameter(s) with correlation to parameter included in regression	Mean distance moved (1)	Supported rearing probability (1)	Unsupported rearing probability (1)	Twitching probability (1)	Grooming probability (1.0)	
	Mean velocity (1)	Sniffing duration (0.4)	Unsupported rearing frequency (0.8)	Sniffing frequency (0.8)		
	Walking duration (0.9)	Sniffing probability (0.4)	Resting probability (0.2)	Supported rearing frequency (0.6)		
	Walking probability (0.9)					
	Walking frequency (0.9)					
	Maximum velocity (0.5)					
	Jumping probability (0.3)					

one representative parameter selected from each domain based on perceived clinical relevance to LBP. These behavioral tests and analysis of behavioral data of experimental and control animals were blinded to the investigators.

2.5 | Serum biomarker analysis

Venous blood samples were obtained from rats at baseline and 1, 6, 12, 18, and 24 weeks post puncture, and serum was immediately isolated and frozen at −80°C until assay. The concentration of serum pain biomarker Neuropeptide Y (NPY) and inflammatory biomarker Regulated on Activation Normal T Cell Expressed and

Presumably Secreted (RANTES) were quantified using ELISA (Cat # EIAR-ProNPY, ELR-RANTES; RayBiotech). Data were reported as a mean ± standard error, and mean values were compared between groups at each timepoint and within each group at each timepoint to baseline.

2.6 | Histology

L2/L3 functional spine units were cut into 6-m thick coronal sections. To maximize consistency, disc tissue sections close to the disc center were stained with hematoxylin and eosin (H&E) by standard procedures and photographed under 20×, 40×, and 100× magnification (Nikon Eclipse E800). Histologic quantitative scoring for IDD was performed by three blinded observers using a previously described scoring system for rodent models.[33] Data were reported as a mean ± standard error.

TABLE 2 Behavioral differences between puncture and control groups using a linear mixed effects regression model

Behavioral parameter	Difference in experimental group compared to controls	p-value
Total distance moved (cm)	−333.5[a]	**0.013**
Supported rearing duration (s)	−14.6	**0.009**
Unsupported rearing duration (s)	−3.7	**0.027**
Twitching frequency (per trial)	−5.7	**0.010**
Grooming duration (s)	25.7	0.26
Grooming frequency (per trial)	2.3	0.34

Note: Bold values represent significance ($p < 0.05$).
[a]Interpretation example: For each trial, individual rats in the experimental group moved on average 333.5 cm less than individual rats in the control group.
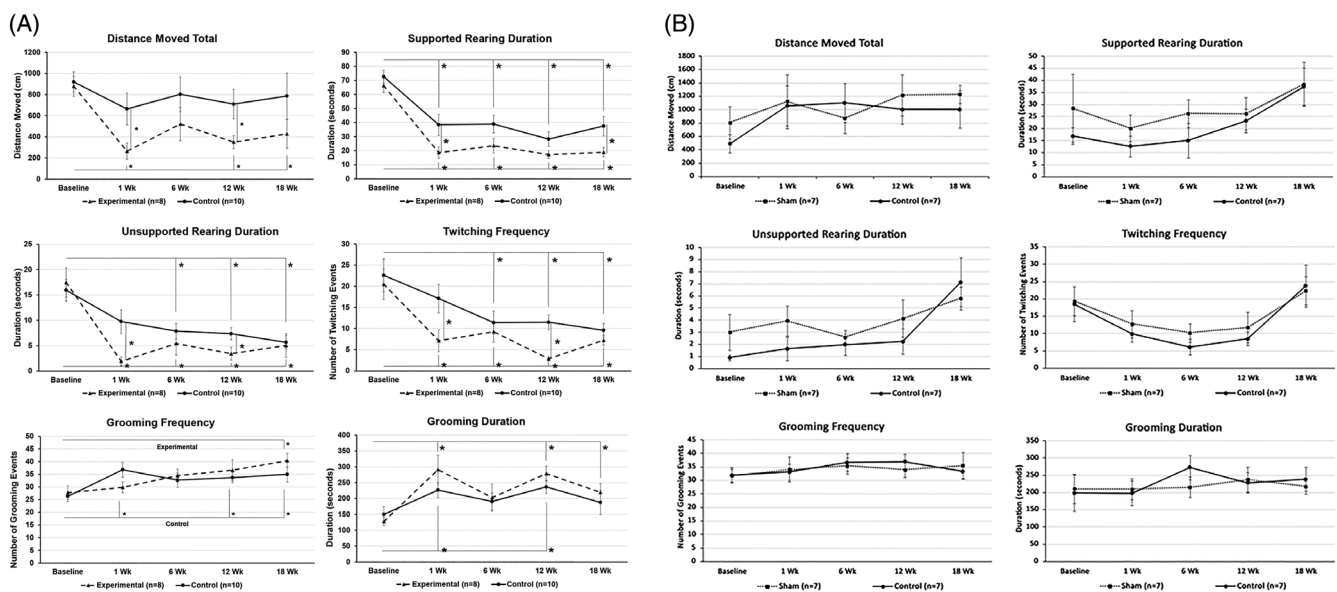
2.7 | Immunohistochemistry

Immunohistochemistry (IHC) was performed on L2/L3 discs using anti-MMP13 (Cat # AB39012; Abcam) and anti-aggrecan (Cat # AB1031; EMD Millipore) antibodies as previously described.[34] Discs were photographed under 20× and 40× magnification (Nikon Eclipse E800). For quantification, all slides were visualized under 40× magnification, and a calculation of the percentage of total NP area showing positive IHC staining was performed using the color deconvolution plugin in Image J software (NIH). Thresholds remained constant for each individual antibody. Data were reported as a mean ± standard error.

FIGURE 4 Rat behaviors assessed by Open Field Assay. Representative behavioral parameters from two separate sets of experiments comparing (A) unstabbed control and experimental groups, and (B) unstabbed control and sham groups. Asterisks represent significant differences ($p < 0.05$) within groups when compared to baseline (indicated by the asterisks above and below the plots) and between groups at the specified timepoint (indicated by the asterisks between the plots). Error bars represent one standard error

2.8 | DMMB assay for total disc glycosaminoglycan

L3/L4 discs were carefully dissected and isolated. NP and AF tissues from each disc were carefully isolated, weighed, and digested using an extracellular matrix digestion buffer containing 1 M NaAcetate, 0.5 M EDTA, 1 M L-cystine, and 60 mg/ml papain dissolved in 55 mM citric acid/150 mM NaCl. Total glycosaminoglycan (GAG) was measured by dimethylmethylene blue (DMMB) assay and normalized to DNA and tissue weight as previously described.[35] Mean ratios were compared between experimental and control groups. DNA/tissue mass ratios were also calculated for each sample and means were compared between groups. Data were reported as a mean ± standard error.

2.9 | Statistical analysis

All quantitative MRI, histologic, biochemical, and serum biomarker data were compared using two-sided Student's t-test. A linear mixed effects regression model was used to compare behavioral parameters. Statistical significance was defined as $p < 0.05$ for all tests.

3 | RESULTS

3.1 | Mortality and morbidity

Two of the 10 experimental rats (20%) unexpectedly died before sacrifice on postoperative day (POD) 6. Death of one of these two dead rats was likely caused by injury-induced intraabdominal bleeding as blood was found in the abdomen at the time of death. Three of the 10 experimental rats (30%) were noted to have gait abnormalities postoperatively. The first animal was noted to have bilateral hindleg weakness on POD 0 with right hindleg weakness resolving by POD 2, but left hindleg weakness continuing until its death on POD 6. The second animal was noted to have left hindleg weakness on POD 1 that resolved by POD 12. The third animal
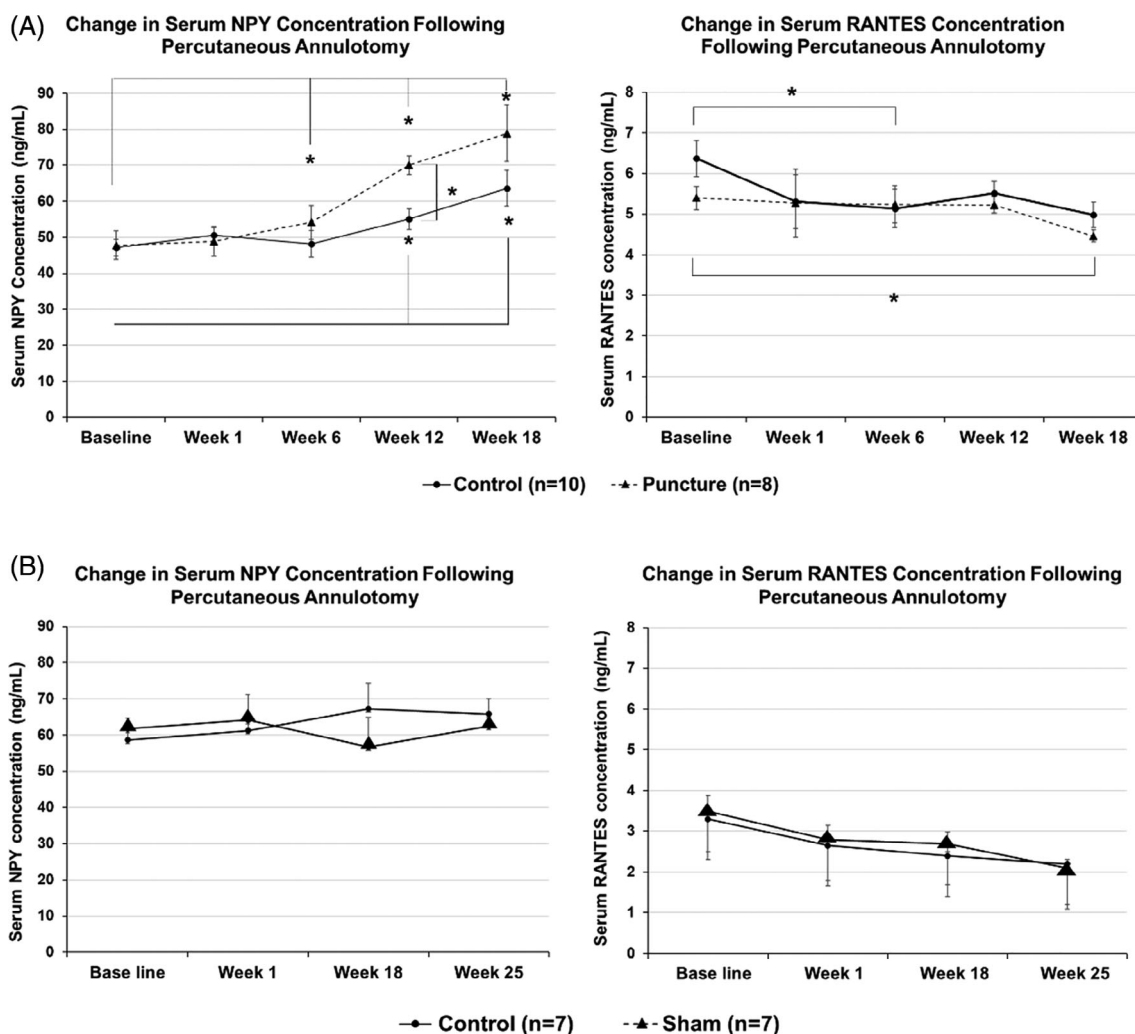

FIGURE 5 Serum concentrations of NPY and RANTES in control and experimental groups (A) and between control and sham groups (B). Asterisks represent significant differences ($p < 0.05$) within groups when compared to baseline (indicated by the asterisks above and below the plots) and between groups at the specified timepoint (indicated by the asterisks between the plots). Error bars represent one standard error. NPY, neuropeptide Y; RANTES, Regulated on Activation Normal T Cell Expressed and Presumably Secreted

developed evidence of slight left leg weakness on POD 5 that resolved by POD 13. There was no permanent deficit noted in any of the rats for behavioral tests at timepoints 6, 12, and 18 weeks post puncture.

3.2 | Magnetic resonance imaging

Loss of MRI T2 disc signal intensity is consistent with a loss of NP water content and disc degeneration.[36,37] Significant decreases from baseline in mean disc signal intensities were noted in punctured discs in the experimental animals at 6, 12, and 18 weeks post puncture (all $p < 0.001$) (Figure 3B). No significant changes in signal intensities from baseline were noted in the control animals. In the experimental group, statistically significant decreases from baseline in mean disc signal intensities were also noted at L1/L2 at 6 weeks ($p = 0.008$) and 12 weeks ($p = 0.003$), and at L5/L6 at 12 weeks ($p = 0.015$) and 18 weeks ($p = 0.03$). Mean disc signal intensities of the punctured discs in the experimental animals (L2/L3, L3/L4, L4/L5) were significantly lower than their unpunctured counterparts in the control animals at all postoperative timepoints (all $p < 0.001$). These MRI results indicate pronounced IDD in rats by week 6 post puncture. No significant differences were noted in the unpunctured discs (L1/L2, L5/L6) of the experimental animals when compared to the same level in the control animals or sham animals (Figure 3C).

3.3 | Behavioral assessments

The principal component analysis identified six distinct domains of related parameters. The representative parameters for each domain with associated parameters are seen in Table 1. The correlation between associated parameters and representative parameters is indicated in parentheses. Supported rearing occurred when the rat reared with forepaw contact against arena walls. Unsupported rearing occurred when the rat reared without forepaw contact against arena walls.[38]

During the 10-min open-field behavioral tests, experimental rats traveled 333.5 cm less per animal per trial than control rats ($p = 0.013$). Experimental rats spent on average 14.6 s less in a supported rearing position per animal per trial ($p = 0.004$) and on average 3.7 s less in an unsupported rearing position per animal per trial ($p = 0.027$) than control rats. Experimental rats twitched on average 5.7 instances less per animal per trial than control rats ($p = 0.017$) (Table 2). Experimental rats groomed on average 2.3 instances more per animal per trial ($p = 0.34$) and spent on average an additional 25.7 s grooming per animal per trial (0.26) than control rats, although these differences failed to reach statistical significance. Detailed results of each representative behavioral parameter are displayed in Figure 4A. Together, these findings suggest that rats which underwent percutaneous lumbar annular puncture displayed greater pain-related behaviors. Notably, sham animal data, which did not

demonstrate the same behavioral changes, were observed in the experimental punctured rats, arguing against changes caused by the needle puncture approach itself (Figure 4B).

3.4 | Serum biomarkers

Neuropeptide Y is a small peptide with known nociceptive functions in the peripheral and central nervous systems, as well as associations with multiple stress-related conditions.[39] RANTES is a chemokine that is upregulated in response to inflammatory stimuli and leads to an increase in catabolic activity.[40] Assessment of these two serum biomarkers was performed in this study because previous work demonstrated an association between serum concentrations of these biomarkers and chronic LBP in humans.[41] Serum NPY concentrations increased in rats post puncture (Figure 5A), as evidenced by the significantly greater NPY levels at the 6-, 12-, and 18-week timepoints compared to baseline values (54.1 vs. 47.8 ng/ml, $p = 0.026$; 70.0 vs. 47.8 ng/ml, $p < 0.001$, and 72.5 ng/ml, $p = 0.018$, respectively). Experimental animals also exhibited higher serum NPY concentrations than control animals at the 6-, 12-, and 18-week timepoints, though this difference only reached statistical significance at the 12-week timepoint (70.0 vs. 55.7 ng/ml, $p = 0.002$). Of note, serum NPY concentrations in the control group also modestly increased at the 12- and 18-week timepoints compared to the baseline value (55.7 vs. 47.1 ng/ml, $p = 0.048$ and 63.6 vs. 47.1 ng/ml, $p = 0.031$, respectively).

No significant differences were found in serum RANTES concentrations between experimental and control groups (Figure 5A). Experimental animals displayed significantly lower serum RANTES concentrations compared to baseline at the 18-week timepoint (4.5 vs. 5.4 ng/ml, $p = 0.012$). Control animals displayed significantly lower serum RANTES concentrations compared to baseline at the 6-week timepoint (5.1 vs. 6.4 ng/ml, $p = 0.011$). Compared to control rats, sham rats

TABLE 3 Histologic grading of intervertebral disc degeneration

	Experimental group ($n = 3$)	Control group ($n = 3$)
NP shape*	2.0 ± 0.00	0.3 ± 0.50
NP area*	1.9 ± 0.33	0.4 ± 0.53
Cell number	1.6 ± 0.73	0.9 ± 0.60
Cell morphology*	2.0 ± 0.00	0.8 ± 0.44
NP/AF border appearance*	2.0 ± 0.00	0.4 ± 0.53
AF lamellar organization*	1.3 ± 0.71	0.2 ± 0.44
AF tears/fissures/disruptions*	1.4 ± 0.53	0.4 ± 0.53
Endplate disruptions/ microfractures and osteophytes/ossification*	1.9 ± 0.33	0.4 ± 0.53
Composite score*	14.1 ± 1.27	4.0 ± 2.45

Note: A higher score indicates a higher degree of disc degeneration.
Abbreviations: AF, annulus fibrosus; NP, nucleus pulposus.
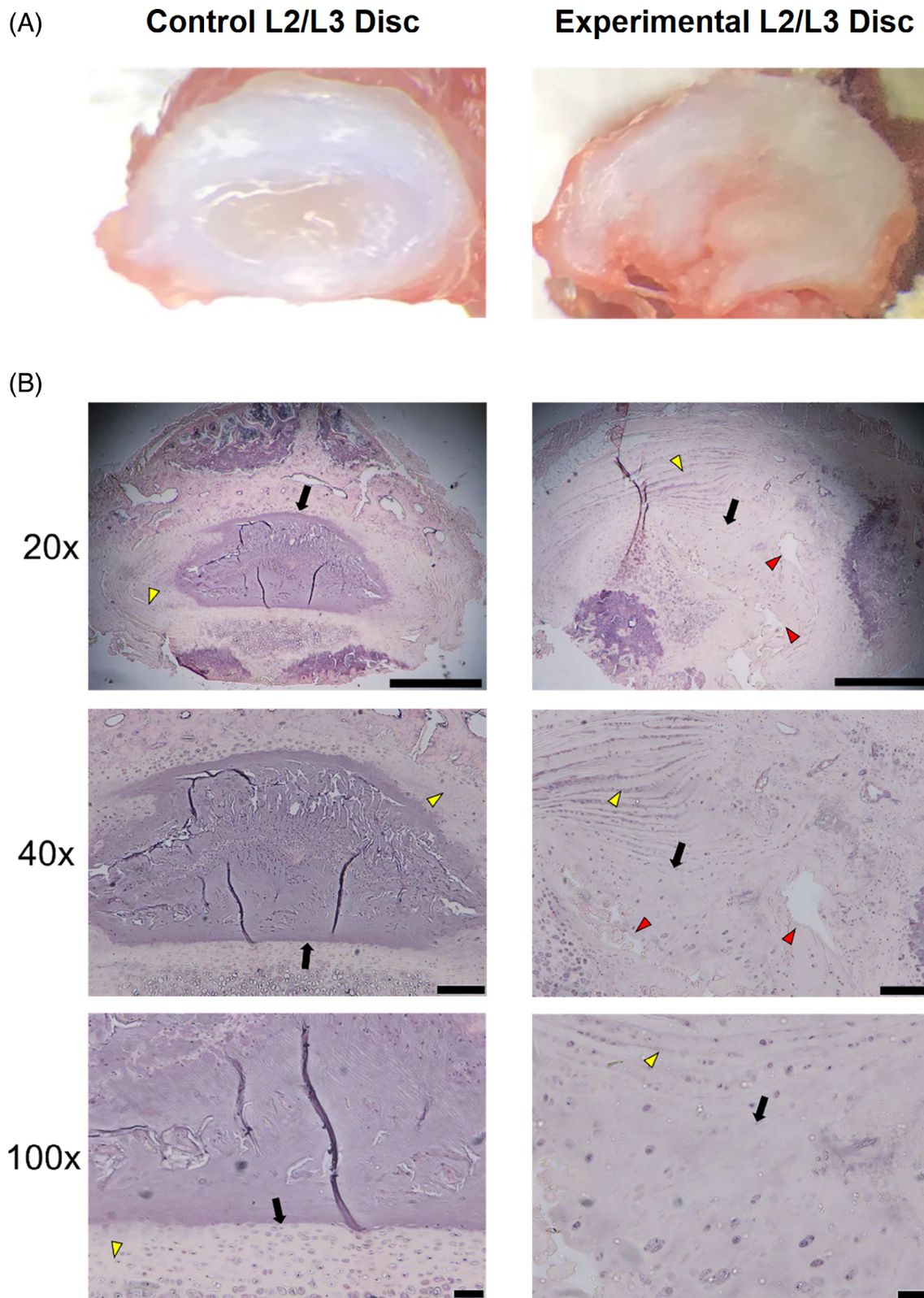*Indicate significant differences between experimental and control groups ($p < 0.05$).

FIGURE 6 Effects of annular puncture on rat disc gross morphology and histological features. (A) Comparison of gross morphology in a control (left) and experimental (right) L2/L3 disc. Punctured discs exhibited loss of hydration and structural organization. Representative 6-μm axial slices of control (left column) and experimental (right column) discs following H&E staining. Images shown at 20× (top row, black scale bar = 500 mm), 40× (middle row, black scale bar = 200 mm), and 100× (bottom row, black scale bar = 60 mm) magnification. Experimental discs show distinct changes in disc architecture, including the loss of a clear NP/AF boundary (black arrows), serpentine AF lamellae (yellow arrowheads), and large fissures/clefts in the NP (red arrowheads). AF, annulus fibrosus; NP, nucleus pulposus
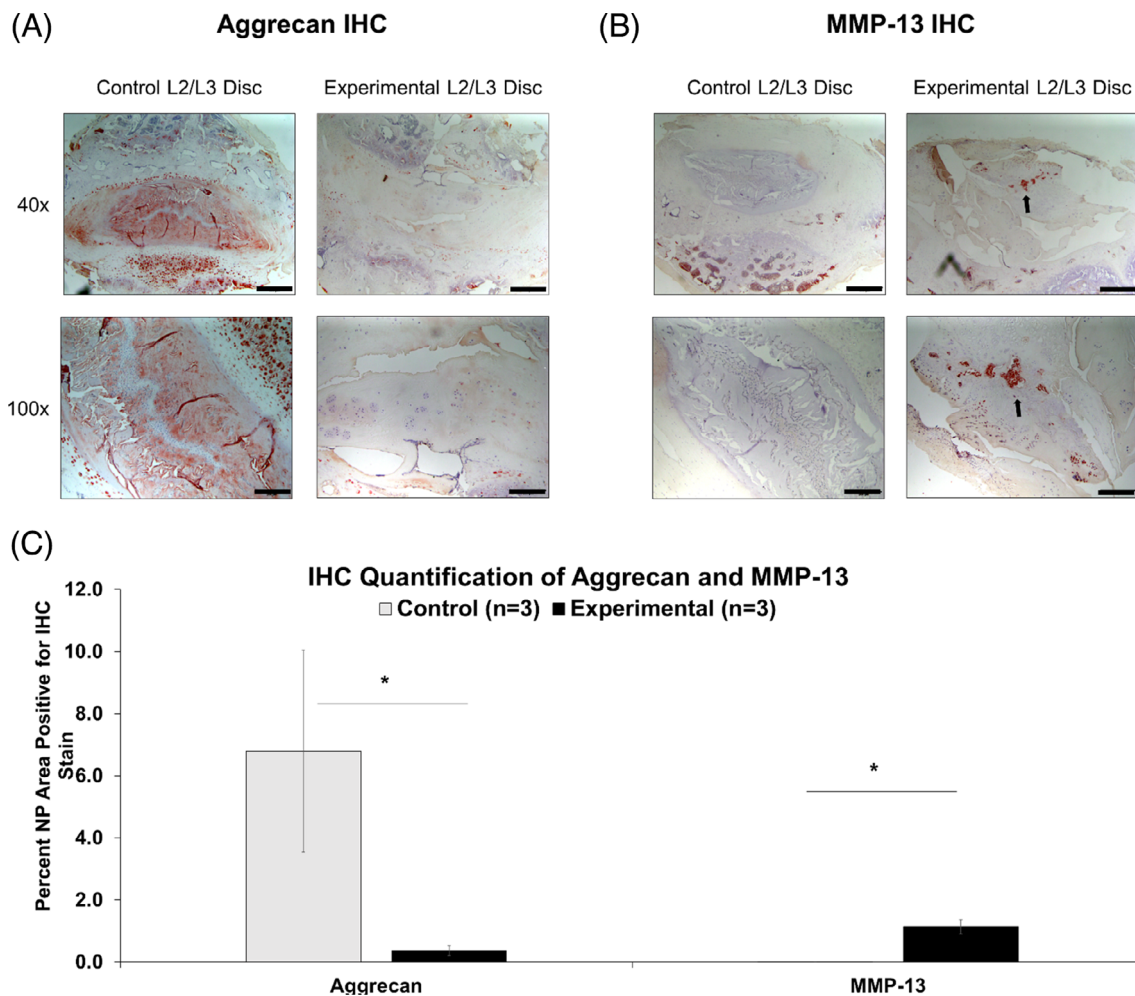
FIGURE 7 Immunohistochemistry. (A) IHC staining for aggrecan (reddish brown) in control (left) and experimental (right) L2/L3 discs. Images shown at 40× (top, black scale bar = 600 mm) and 100× (bottom, black scale bar = 200 mm) magnification. (B) IHC staining for MMP-13 (reddish brown) in control (left) and experimental (right) L2/L3 discs. Representative discs from four individual animals, two control (left) and two experimental (right), are shown in this Figure. (C) Quantification of IHC staining revealed a smaller percentage of NP area positive for aggrecan (left) and a greater percentage of NP area positive for MMP-13 (right) in the punctured discs. Error bars represent one standard error. IHC, immunohistochemistry; NP, nucleus pulposus

also exhibited no significant differences between serum RANTES and NPY concentrations at the different timepoints post surgery (Figure 5B).

3.5 | Gross appearance and histology

Gross evaluation of punctured L2/L3 discs in experimental rats revealed apparent dehydration and fibrosis of the NP when compared to unpunctured L2/L3 discs in control rats (Figure 6A). Hematoxylin and eosin staining revealed considerable degenerative changes (Figure 6B). These findings were confirmed by blinded scoring using the histological grading system developed by Lai et al.[33] The experimental group had significantly higher composite scores, which indicates changes consistent with IDD (14.1 vs. 4.0) (Table 3). In the experimental group, there was a significant loss of NP shape (2.0 vs. 0.3, $p = 0.01$) and area (1.9 vs. 0.4, $p = 0.04$) in the NP, significantly

greater disorganization (1.4 vs. 0.4, $p = 0.03$) in the AF, and a significant loss of a clear NP/AF boundary (2.0 vs 0.4, $p < 0.001$).

3.6 | Immunohistochemistry

To confirm the loss of disc proteoglycan content and upregulation of mediators of matrix degradation, we performed immunohistochemical staining for disc aggrecan (Figure 7A) and MMP-13 (Figure 7B). Quantification of IHC staining revealed a significantly greater percentage of total NP area staining positive for MMP-13 in punctured discs (1.14% vs. 0.01%, $p = 0.008$), and a lower percentage of total NP area positive for aggrecan in the punctured discs (0.36% vs. 6.80%, $p = 0.12$) (Figure 7C). Thus, rats with annular puncture exhibited loss of proteoglycan and gain of the catabolic enzyme MMP-13 in their injury-induced degenerative discs.
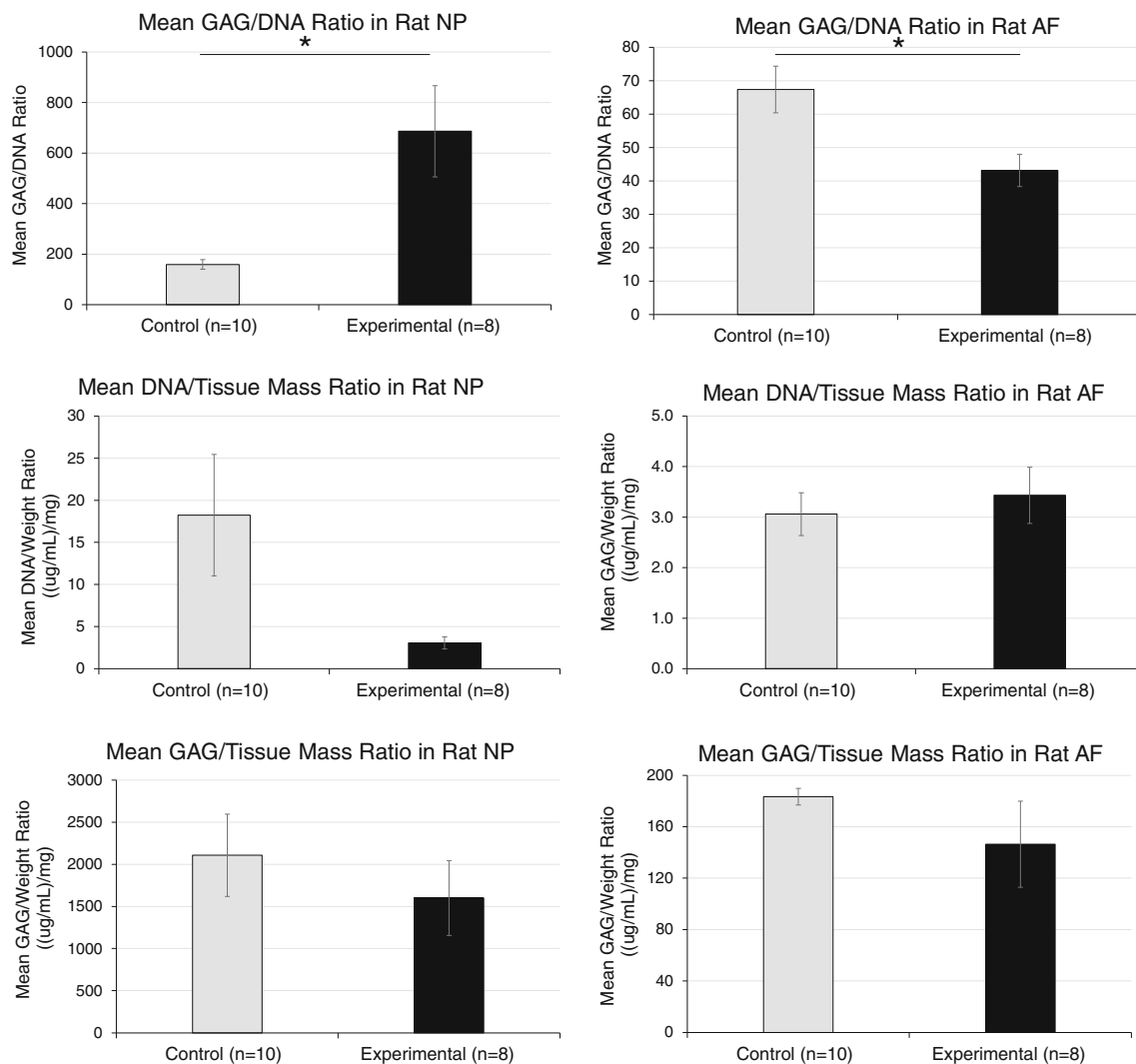
FIGURE 8 GAG content in control and experimental animal NP (left) and AF (right), as standardized to DNA content (top) and tissue mass (bottom). DNA content is also shown standardized to tissue mass (middle). Error bars represent one standard error. AF, annulus fibrosus; GAG, glycosaminoglycan; NP, nucleus pulposus

3.7 | GAG assay

Glycosaminoglycan analysis using DMMB assay revealed a significantly higher GAG/DNA ratio in experimental NP when compared to control NP (686.5 vs. 159.4, $p = 0.022$) in the L3/4 disc (Figure 8, top). This finding was likely driven by lower concentrations of DNA in the experimental NP due to cell loss rather than an increase in GAG in experimental discs, as the DNA/Tissue Mass ratio in experimental NP was appreciably lower than the ratio in the control NP (3.07 [μg/ml]/mg vs. 18.23 [μg/ml]/mg, $p = 0.065$). Experimental NP also exhibited a lower GAG/Tissue Mass ratio than control NP (1601.0 [μg/ml]/mg vs. 2107.6 [μg/ml]/mg, $p = 0.454$). Overall, the DMMB result supports evidence of loss of NP cells and proteoglycan matrix that is consistent with disc degeneration.

In the AF, the experimental group exhibited a significantly lower GAG/DNA ratio than controls (43.2 vs. 67.4, $p = 0.015$) (Figure 8, bottom). There were no differences between groups in the

DNA/Tissue Mass ratio (3.4 [μg/ml]/mg vs. 3.1 [μg/ml]/mg, $p = 0.59$) or the GAG/Tissue Mass ratio (146.5 [μg/ml]/mg vs. 183.5 [μg/ml]/mg, $p = 0.25$).

4 | DISCUSSION

This study is the first to successfully induce IDD in the rat lumbar spine through a purely percutaneous technique, which minimizes the morbidity inherent to open exposures. Furthermore, rats exhibited measurable differences in pain-related behaviors when compared to control animals. The coexistence of these behaviors with IDD was validated through a variety of independent assays, including imaging, histologic, and biochemical data.

While open approaches facilitate lumbar disc puncture, there are several associated complications. For ventral open approaches, retraction and extracorporeal reflection of the bowel has a high risk of

gastrointestinal distress.[19,21] Additionally, dissection straying over 1.5 mm from the midline can result in neurologic complications in as many as 70% of subjects.[19] Li et al. hoped to avoid these issues by using a posterior approach.[20] Like the current model, they utilized intraoperative fluoroscopy to guide needle punctures. However, the technique still required an open incision and dissection of paraspinal musculature to access the disc space.

Our procedure had a mortality rate of 20%, which is slightly higher than the 11.6% reported by Damle et al.[19] Of note, Damle et al. initially had a comparable mortality rate of 19.6%, when removing the cecum and small intestine from the abdomen as originally described.[19,21] After performing the procedure on a total of 258 rats, they demonstrated marked improvement in their technique and mortality rate. Although our incidence of postoperative neurologic deficit (30%) is higher than that found by Damle et al. (10.9%), all deficits are resolved by 2 weeks postoperatively.[19] Thus, the observed behavioral changes seen at 6-, 12-, and 18-week timepoints were not attributable to neurologic deficits. The cause of our 20% mortality rate was likely due to injury originating from the puncturing procedure which was not fully refined in our initial batch of experimental rats. This percutaneous technique requires a certain degree of technical skills and optimization which we have since further refined to reduce mortality and morbidity to 5%–10%. We continue to further refine our percutaneous annular puncture technique to decrease mortality and morbidity to a minimum.

Various independent experiments were performed to confirm IDD in our model. DSI fiber tracking software, which has previously been used for neuronal mapping, accurately quantifies MRI NP signal intensity and voxel count.[42–44] Our results revealed NP signal loss in experimental discs that were not present in controls. Previous studies have correlated a decrease in MRI T2 signal intensity with an increased histologic grade of disc degeneration.[36,45–47] These findings provide in vivo evidence of IDD at the earliest measured timepoint (6 weeks) that persisted throughout the 18-week duration of the study. Though statistically significant decreases in MRI signal intensity were also noted in the unpunctured L1/L2 and L5/L6 discs in the experimental animals, the magnitude of these changes was substantially smaller than those seen in the punctured discs and may represent accelerated age-related changes related to systemic effects of the disc puncture or a local inflammatory process in paraspinal tissues related to the needle puncture, as this was not observed in the control animals.

Experimental animals had significantly higher histologic disc degenerative grades than controls, showing distinct disruption of disc architecture, a loss of hydration, loss of demarcation between the AF and NP, and tissue discoloration in the experimental discs. These gross and histological differences between experimental and control discs were consistent with previous studies,[11,48] Proteoglycan breakdown and upregulation of catabolic enzymes such as matrix metalloproteinases (MMPs) are common features in IDD.[10,48–52] IHC staining for aggrecan was considerably decreased in experimental NP, consistent with prior studies showing decreased proteoglycan content in degenerated discs.[18,53,54] Additionally, IHC staining for MMP-13

was readily detectable in experimental NP, but was not apparent in control NP, which is consistent with the findings of Le Maitre et al., who noted that MMP-13 expression was much more common in degenerative discs, with cells expressing MMP-13 primarily located in the NP.[51]

Prior studies have noted that disc degeneration is associated with decreased GAG content.[18,35,55,56] When normalized to tissue mass, our model shows a decrease in the GAG content of the NP and AF in the experimental group, although these differences failed to reach significance. When normalized to DNA content, the AF of the experimental group showed a significantly lower GAG content than the controls. Interestingly, the NP of the experimental group showed a significantly higher GAG/DNA ratio, mainly due to loss of cellularity as evidenced by a sizeable decrease in the DNA/tissue mass ratio in the experimental group. Furthermore, a quantitative decrease in NP DNA is consistent with our histologic findings showing a considerable loss of NP cellularity in the experimental group. These findings are consistent with disc degeneration as observed in other animal models and humans.

In addition to biochemical changes within IVDs, prior studies have identified relationships between serum biomarkers (including NPY and RANTES) and musculoskeletal disorders, including back pain.[41,57–60] NPY and RANTES are both expressed by the IVD and are associated with symptomatic LBP in humans.[41,61–64] Our results showed consistently higher serum concentrations of NPY in the experimental group compared to the control or sham groups beginning 6 weeks after the annular puncture, consistent with prior research associating higher levels of serum NPY with symptomatic back pain.[41] However, this difference only reached significance at the 12-week postoperative timepoint. There was an increase in serum NPY concentrations in the control group at the 12- and 18-week timepoints compared to baseline, which could be related to either aging or stress of other experimental procedures (i.e. transport, MRIs, and behavioral tests). Serum RANTES concentrations were similar between the experimental and control groups and showed a relatively constant value over time until the 18-week timepoint, which may suggest a lack of persistent systemic inflammation in this model.

Characterizing pain in animal models is difficult, and numerous techniques for measuring pain-related behaviors in animals have been developed.[65] Open-field testing has been utilized in prior studies to characterize spontaneous pain behaviors.[29,66–69] Historically, "exploratory" behavior was measured by calculating the number of unique areas that an animal visited.[68] More recent advancements have found relationships between other behaviors, including grooming and "wet-dog shakes," and IVD puncture.[29,67] The behavioral changes found in the current study are consistent with prior findings. Cho et al. found a decrease in total distance moved and rearing behaviors in rats exposed to painful stimuli, and Olmarker identified a significant increase in grooming behaviors following IVD puncture.[29,69] We observed a similar increase in both the frequency and duration of grooming in experimental animals, although this failed to reach statistical significance. Though Olmarker identified an increase in "wet-dog shakes" in experimental animals, the current study did not specifically track this behavior.[29] In the current

study, a principal component analysis was utilized to identify groups of highly correlated behaviors and thus focus on the most relevant comparisons between the experimental and control groups. Representative behavioral parameters in each group were selected based upon perceived relevance to discogenic LBP as supported by prior literature. To minimize potential behavioral differences in sexes in response to LBP, the current study included only male rats.[70]

Our rat model has several limitations. First, it does not model slow progressive IDD but rather mimics a rapid injury-induced disc degeneration from the use of a relatively larger needle (23-gauge) and extensive movement of the needle to maximize disc tissue disruption. The use of a smaller needle may facilitate the development of a model of slower progressing IDD. Second, it is not possible to ascertain whether the observed behavioral changes in our experimental rats were due to discogenic back pain or neuropathic pain secondary to iatrogenic nerve root injury. However, all postoperative neurological deficits were resolved at the latest by POD 13. Although meticulous attempts were made to control the depth of puncture, fluoroscopy is unable to visualize the IVD and as a result, the contralateral AF may have been damaged during the procedure. Additionally, the L5/L6 and L6/S1 discs are obstructed by the iliac crest, and therefore, this approach would not be feasible to puncture all discs of the lumbar spine. Mechanisms driving pain in our rat model were not explored as we did not assess DRG changes or disc neoinnervation and neovascularization which might enhance sensitization of disc peripheral neurons. Importantly, it was the intent of this study to evaluate the functional response to the injury-induced degeneration, which informed the selection of the open-field mobility assessments.[71,72] Previous studies have validated and used measures of central sensitization, such as hind paw thermal and mechanical sensitivity[73,74] which were not measured in the current study. Future studies would benefit from combining these types of pain assessments to glean a more comprehensive view of LBP in rodent models. Finally, only male rats were used, but future investigation using both male and female rats is needed to identify any relevant molecular and behavioral differences that may result from the differences in IDD and functional healing responses between the sexes, which have been reported.[73] Nonetheless, this is the first reported reproducible rodent model of IDD and back pain via percutaneous lumbar annular puncture with associated behavioral changes that can be used to study the biology of IDD as well as test therapeutics to treat IDD.

AUTHOR CONTRIBUTIONS

Richard A. Wawrose, Brandon K. Couch, Malcom Dombrowski, Stephen R. Chen, Anthony Oyekan, and Dong Wang performed the percutaneous lumbar punctures. Richard A. Wawrose, Brandon K. Couch, Malcom Dombrowski, Stephen R. Chen, Marit Johnson, T. Kevin Hitchens, and Tao Jin performed MRI imaging. Richard A. Wawrose, Brandon K. Couch, Marit Johnson, Stephen R. Chen, Anthony Oyekan, Joseph Chen, Karthik Modali, Zachary Sedor-Schiffhauer performed the behavioral analyses. Qing Dong, Dong Wang, and Chaoming Zhou performed the serum biomarker analyses, histology, and immunohistochemistry. Kevin M. Bell, Joon Y. Lee, Gwendolyn A. Sowa, and Nam V. Vo were responsible for research design. Data analysis and interpretation was performed by all authors. All authors have read and approved the final submitted manuscript.

CONFLICT OF INTEREST

The authors declare no conflicts of interest.

ORCID

Stephen R. Chen https://orcid.org/0000-0001-7000-9842
Anthony Oyekan https://orcid.org/0000-0002-9155-1283

REFERENCES

1. Vos T, Abajobir AA, Abate KH, et al. Global, regional, and national incidence, prevalence, and years lived with disability for 328 diseases and injuries for 195 countries, 1990–2016: a systematic analysis for the global burden of disease study 2016. *Lancet*. 2017;*390*(10100):1211-1259.
2. Goode AP, Carey TS, Jordan JM. Low back pain and lumbar spine osteoarthritis: how are they related? *Curr Rheumatol Rep*. 2013;*15*(2):305.
3. US Burden of Disease Collaborators, Mokdad H, Ballestros K, et al. The state of US health, 1990–2016: burden of diseases, injuries, and risk factors among US states. *JAMA*. 2018;*319*(14):1444-1472.
4. Katz JN. Lumbar disc disorders and low-back pain: socioeconomic factors and consequences. *J Bone Joint Surg Am*. 2006;*88*(Suppl 2):21-24.
5. Dagenais S, Caro J, Haldeman S. A systematic review of low back pain cost of illness studies in the United States and internationally. *Spine J*. 2008;*8*(1):8-20.
6. Itoh H, Kitamura F, Yokoyama K. Estimates of annual medical costs of work-related low back pain in Japan. *Ind Health*. 2013;*51*(5):524-529.
7. Geurts JW, Willems PC, JaKallewaard JW, et al. The impact of chronic discogenic low back pain: costs and patients' burden. *Pain Res Manag*. 2018;*2018*:4696180.
8. Schwarzer AC, Aprill CN, Derby R, Fortin J, Kine G, Bogduk N. The prevalence and clinical features of internal disc disruption in patients with chronic low back pain. *Spine (Phila Pa 1976)*. 1995;*20*(17):1878-1883.
9. DePalma MJ, Ketchum JM, Saullo T. What is the source of chronic low back pain and does age play a role? *Pain Med*. 2011;*12*(2):224-233.
10. Vo NV, Hartman RA, Patil PR, et al. Molecular mechanisms of biological aging in intervertebral discs. *J Orthop Res*. 2016;*34*(8):1289-1306.
11. Peng BG. Pathophysiology, diagnosis, and treatment of discogenic low back pain. *World J Orthop*. 2013;*4*(2):42-52.
12. Daly C, Ghosh P, Jenkin G, et al. A review of animal models of intervertebral disc degeneration: pathophysiology, regeneration, and translation to the clinic. *Biomed Res Int*. 2016;*2016*:5952165.
13. Xi Y, Kong J, Liu Y, et al. Minimally invasive induction of an early lumbar disc degeneration model in rhesus monkeys. *Spine (Phila Pa 1976)*. 2013;*38*(10):E579-E586.
14. Luo TD, Marquez-Lara A, Zabarsky ZK, et al. A percutaneous, minimally invasive annulus fibrosus needle puncture model of intervertebral disc degeneration in rabbits. *J Orthop Surg (Hong Kong)*. 2018;*26*(3):2309499018792715.

15. Zhang H, la Marca F, Hollister SJ, Goldstein SA, Lin CY. Developing consistently reproducible intervertebral disc degeneration at rat caudal spine by using needle puncture. *J Neurosurg Spine*. 2009;*10*(6): 522-530.

16. Rousseau MA, Ulrich JA, Elisa Bass EC, et al. Stab incision for inducing intervertebral disc degeneration in the rat. *Spine (Phila Pa 1976)*. 2007;*32*(1):17-24.

17. Jeong JH, Jin ES, Min JK, et al. Human mesenchymal stem cells implantation into the degenerated coccygeal disc of the rat. *Cytotechnology*. 2009;*59*(1):55-64.

18. Han B, Zhu K, Li FC, et al. A simple disc degeneration model induced by percutaneous needle puncture in the rat tail. *Spine (Phila Pa 1976)*. 2008;*33*(18):1925-1934.

19. Damle SR, Krzyzanowska A, Frawley RJ, Cunningham ME. Surgical anatomy, transperitoneal approach, and early postoperative complications of a ventral lumbar spine surgical model in Lewis rats. *Comp Med*. 2013;*63*(5):409-415.

20. Li D, Yang H, Huang Y, Wu Y, Sun T, Li X. Lumbar intervertebral disc puncture under C-arm fluoroscopy: a new rat model of lumbar intervertebral disc degeneration. *Exp Anim*. 2014;*63*(2):227-234.

21. Rousseau MA, Bass EC, Lotz JC. Ventral approach to the lumbar spine of the Sprague-Dawley rat. *Lab Anim (NY)*. 2004;*33*(6): 43-45.

22. Lai A, Moon A, Purmessur D, et al. Annular puncture with tumor necrosis factor-alpha injection enhances painful behavior with disc degeneration in vivo. *Spine J*. 2016;*16*(3):420-431.

23. Glaeser JD, Tawackoli W, Ju DG, et al. Optimization of a rat lumbar IVD degeneration model for low back pain. *JOR Spine*. 2020;*3*(2):e1092.

24. Lai A, Moon A, Purmessur D, et al. Assessment of functional and behavioral changes sensitive to painful disc degeneration. *J Orthop Res*. 2015;*33*(5):755-764.

25. Evashwick-Rogler TW, Lai A, Watanabe H, et al. Inhibiting tumor necrosis factor-alpha at time of induced intervertebral disc injury limits long-term pain and degeneration in a rat model. *JOR Spine*. 2018;*1*(2):e1014.

26. Leimer EM, Gayoso MG, Jing L, Tang SY, Gupta MC, Setton LA. Behavioral compensations and neuronal remodeling in a rodent model of chronic intervertebral disc degeneration. *Sci Rep*. 2019; *9*(1):3759.

27. Vieira JO, Duarte JO, Costa-Ferreira W, Morais-Silva G, Marin MT, Crestani CC. Sex differences in cardiovascular, neuroendocrine and behavioral changes evoked by chronic stressors in rats. *Prog Neuropsychopharmacol Biol Psychiatry*. 2018;*81*:426-437.

28. Hennig J, Nauerth A, Friedburg H. RARE imaging: a fast imaging method for clinical MR. *Magn Reson Med*. 1986;*3*(6):823-833.

29. Olmarker K. Puncture of a lumbar intervertebral disc induces changes in spontaneous pain behavior: an experimental study in rats. *Spine (Phila Pa 1976)*. 2008;*33*(8):850-855.

30. Sharon G, Cruz NJ, Kang DW, et al. Human gut microbiota from autism Spectrum disorder promote behavioral symptoms in mice. *Cell*. 2019;*177*(6):1600-1618.e17.

31. Phillips KF, Santos E, Blair RE, Deshpande LS. Targeting intracellular calcium stores alleviates neurological morbidities in a DFP-based rat model of gulf war illness. *Toxicol Sci*. 2019;*169*(2):567-578.

32. Iturra-Mena AM, Aguilar-Rivera M, Arriagada-Solimano M, Pérez-Valenzuela C, Fuentealba P, Dagnino-Subiabre A. Impact of stress on gamma oscillations in the rat nucleus accumbens during spontaneous social interaction. *Front Behav Neurosci*. 2019;*13*:151.

33. Lai A, Gansau J, Gullbrand SE, et al. Development of a standardized histopathology scoring system for intervertebral disc degeneration in rat models: an initiative of the ORS spine section. *JOR Spine*. 2021; *4*(2):e1150.

34. Patil P, Dong Q, Wang D, et al. Systemic clearance of p16(INK4a)-positive senescent cells mitigates age-associated intervertebral disc degeneration. *Aging Cell*. 2019;*18*(3):e12927.

35. Wang D, Nasto LA, Roughley P, et al. Spine degeneration in a murine model of chronic human tobacco smokers. *Osteoarthritis Cartilage*. 2012;*20*(8):896-905.

36. Piazza M, Peck SH, Gullbrand SE, et al. Quantitative MRI correlates with histological grade in a percutaneous needle injury mouse model of disc degeneration. *J Orthop Res*. 2018;*36*(10):2771-2779.

37. Pfirrmann CW, Metzdorf A, Zanetti M, et al. Magnetic resonance classification of lumbar intervertebral disc degeneration. *Spine (Phila Pa 1976)*. 2001;*26*(17):1873-1878.

38. Sturman O, Germain PL, Bohacek J. Exploratory rearing: a context- and stress-sensitive behavior recorded in the open-field test. *Stress*. 2018;*21*(5):443-452.

39. Dombrowski ME, Olsen AS, Vaudreuil N, et al. Rabbit annulus Fibrosus cells express neuropeptide Y, which is influenced by mechanical and inflammatory stress. *Neurospine*. 2020;*17*(1):69-76.

40. Khan AN, Jacobsen HE, Khan J, et al. Inflammatory biomarkers of low back pain and disc degeneration: a review. *Ann N Y Acad Sci*. 2017; *1410*(1):68-84.

41. Sowa GA, Perera S, Bechara B, et al. Associations between serum biomarkers and pain and pain-related function in older adults with low back pain: a pilot study. *J Am Geriatr Soc*. 2014;*62*(11):2047-2055.

42. Yeh FC, Zaydan IM, Suski VR, et al. Differential tractography as a track-based biomarker for neuronal injury. *Neuroimage*. 2019;*202*:116131.

43. Yeh FC, Verstynen TD, Wang Y, Fernández-Miranda JC, Tseng WYI. Deterministic diffusion fiber tracking improved by quantitative anisotropy. *PLoS One*. 2013;*8*(11):e80713.

44. Yeh FC, Tseng WY. NTU-90: a high angular resolution brain atlas constructed by q-space diffeomorphic reconstruction. *Neuroimage*. 2011; *58*(1):91-99.

45. Grunert P, Hudson KD, Macielak MR, et al. Assessment of intervertebral disc degeneration based on quantitative magnetic resonance imaging analysis: an in vivo study. *Spine (Phila Pa 1976)*. 2014; *39*(6):E369-E378.

46. Chai JW, Kang HS, Lee JW, Kim SJ, Hong SH. Quantitative analysis of disc degeneration using axial T2 mapping in a percutaneous annular puncture model in rabbits. *Korean J Radiol*. 2016;*17*(1):103-110.

47. Ohnishi T, Sudo H, Iwasaki K, Tsujimoto T, Ito YM, Iwasaki N. In vivo mouse intervertebral disc degeneration model based on a new histological classification. *PLoS One*. 2016;*11*(8):e0160486.

48. Roughley PJ. Biology of intervertebral disc aging and degeneration: involvement of the extracellular matrix. *Spine (Phila Pa 1976)*. 2004; *29*(23):2691-2699.

49. Roberts S, Caterson B, Menage J, Evans EH, Jaffray DC, Eisenstein SM. Matrix metalloproteinases and aggrecanase: their role in disorders of the human intervertebral disc. *Spine (Phila Pa 1976)*. 2000;*25*(23):3005-3013.

50. Le Maitre CL, Freemont AJ, Hoyland JA. Accelerated cellular senescence in degenerate intervertebral discs: a possible role in the pathogenesis of intervertebral disc degeneration. *Arthritis Res Ther*. 2007;*9*(3):R45.

51. Le Maitre CL, Freemont AJ, Hoyland JA. Localization of degradative enzymes and their inhibitors in the degenerate human intervertebral disc. *J Pathol*. 2004;*204*(1):47-54.

52. Xu H, Mei Q, Xu B, Liu G, Zhao J. Expression of matrix metalloproteinases is positively related to the severity of disc degeneration and growing age in the east Asian lumbar disc herniation patients. *Cell Biochem Biophys*. 2014;*70*(2):1219-1225.

53. Norcross JP, Lester GE, Weinhold P, Dahners LE. An in vivo model of degenerative disc disease. *J Orthop Res*. 2003;*21*(1):183-188.

54. Keorochana G, Johnson JS, Taghavi CE, et al. The effect of needle size inducing degeneration in the rat caudal disc: evaluation using radiograph, magnetic resonance imaging, histology, and immunohistochemistry. *Spine J*. 2010;*10*(11):1014-1023.

55. Nasto LA, Ngo K, Leme AS, et al. Investigating the role of DNA damage in tobacco smoking-induced spine degeneration. *Spine J*. 2014; *14*(3):416-423.

56. Farndale R, Buttle D, Barrett A. Improved quantitation and discrimination of sulphated glycosaminoglycans by use of dimethylmethylene blue. *Biochimica et Biophysica Acta (BBA) - General Subjects*. 1986; *883*(2):173-177.

57. Schell E, Theorell T, Hasson D, Arnetz B, Saraste H. Stress biomarkers' associations to pain in the neck, shoulder and back in healthy media workers: 12-month prospective follow-up. *Eur Spine J*. 2008;*17*(3): 393-405.

58. Goode AP, Schwartz TA, Kraus VB, et al. Inflammatory, structural, and pain biochemical biomarkers may reflect radiographic disc space narrowing: the Johnston County osteoarthritis project. *J Orthop Res*. 2020;*38*(5):1027-1037.

59. Alaaeddine N, Olee T, Hashimoto S, Creighton-Achermann L, Lotz M. Production of the chemokine RANTES by articular chondrocytes and role in cartilage degradation. *Arthritis Rheum*. 2001;*44*(7):1633-1643.

60. Felson DT. The sources of pain in knee osteoarthritis. *Curr Opin Rheumatol*. 2005;*17*(5):624-628.

61. Kepler CK, Markova DZ, Dibra F, et al. Expression and relationship of proinflammatory chemokine RANTES/CCL5 and cytokine IL-1beta in painful human intervertebral discs. *Spine (Phila Pa 1976)*. 2013;*38*(11): 873-880.

62. Ashton IK, Roberts S, Jaffray DC, Polak JM, Eisenstein SM. Neuropeptides in the human intervertebral disc. *J Orthop Res*. 1994;*12*(2): 186-192.

63. Dombrowski ME, Rynearson B, LeVasseur C, et al. ISSLS prize in bioengineering science 2018: dynamic imaging of degenerative spondylolisthesis reveals mid-range dynamic lumbar instability not evident on static clinical radiographs. *Eur Spine J*. 2018;*27*(4): 752-762.

64. Li H, Zou X, Baatrup A, Lind M, Bünger C. Cytokine profiles in conditioned media from cultured human intervertebral disc tissue. Implications of their effect on bone marrow stem cell metabolism. *Acta Orthop*. 2005;*76*(1):115-121.

65. Mosley GE, Evashwick-Rogler TW, Lai A, Iatridis JC. Looking beyond the intervertebral disc: the need for behavioral assays in models of discogenic pain. *Ann N Y Acad Sci*. 2017;*1409*(1): 51-66.

66. Parent AJ, Beaudet N, Beaudry H, et al. Increased anxiety-like behaviors in rats experiencing chronic inflammatory pain. *Behav Brain Res*. 2012;*229*(1):160-167.

67. Olmarker K, Storkson R, Berge OG. Pathogenesis of sciatic pain: a study of spontaneous behavior in rats exposed to experimental disc herniation. *Spine (Phila Pa 1976)*. 2002;*27*(12):1312-1317.

68. Denenberg VH. Open-field behavior in the rat: what does it mean? *Ann N Y Acad Sci*. 1969;*159*(3):852-859.

69. Cho H et al. Voluntary movements as a possible non-reflexive pain assay. *Mol Pain*. 2013;*9*:25.

70. Mosley GE, Hoy RC, Nasser P, et al. Sex differences in rat intervertebral disc structure and function following annular puncture injury. *Spine (Phila Pa 1976)*. 2019;*44*(18):1257-1269.

71. Urban R, Scherrer G, Goulding EH, Tecott LH, Basbaum AI. Behavioral indices of ongoing pain are largely unchanged in male mice with tissue or nerve injury-induced mechanical hypersensitivity. *Pain*. 2011; *152*(5):990-1000.

72. Carola V, D'Olimpio F, Brunamonti E, Mangia F, Renzi P. Evaluation of the elevated plus-maze and open-field tests for the assessment of anxiety-related behaviour in inbred mice. *Behav Brain Res*. 2002; *134*(1–2):49-57.

73. Mosley GE, Wang M, Nasser P, et al. Males and females exhibit distinct relationships between intervertebral disc degeneration and pain in a rat model. *Sci Rep*. 2020;*10*(1):15120.

74. Lai A, Ho L, Evashwick-Rogler TW, et al. Dietary polyphenols as a safe and novel intervention for modulating pain associated with intervertebral disc degeneration in an in-vivo rat model. *PLoS One*. 2019; *14*(10):e0223435.